

¹ The Evolution of Siphonophore Tentilla as Specialized Tools for Prey Capture

³ Alejandro Damian-Serrano^{1,‡}, Steven H.D. Haddock², Casey W. Dunn¹

⁴ ¹ Yale University, Department of Ecology and Evolutionary Biology, 165 Prospect St.,
⁵ New Haven, CT 06520, USA

⁶ ² Monterey Bay Aquarium Research Institute, 7700 Sandholdt Rd., Moss Landing, CA
⁷ 95039, USA

⁸ [‡] Corresponding author: Alejandro Damian-Serrano, email: alejandro.damianserrano@
⁹ yale.edu

¹⁰ Abstract

¹¹ Predators have evolved dedicated body parts to capture and subdue prey. As a clade
¹² of predators specialize in distinct prey taxa, their tools for prey capture diversify into a
¹³ variety of adaptive forms. Studying the evolution of predation is facilitated by a predator
¹⁴ clade with structures used exclusively for prey capture and with significant morphological
¹⁵ variation. Siphonophores, a clade of colonial cnidarians, satisfy these criteria particularly
¹⁶ well, capturing prey with their tentilla (tentacle side branches). Earlier work has shown
¹⁷ that extant siphonophore diets correlate with the different morphologies and sizes of their
¹⁸ tentilla and nematocysts. We hypothesize that evolutionary specialization on different prey
¹⁹ types has driven the phenotypic evolution of these characters. To test this hypothesis, we:
²⁰ (1) measured multiple morphological characters from siphonophore tentacle specimens, (2)
²¹ mapped these data to a phylogenetic tree of 45 species, and (3) analyzed the evolutionary
²² associations between morphological characters and prey type data from the literature. Our
²³ results show that the siphonophore tentillum morphology has strong evolutionary associations
²⁴ with prey type specialization, and suggest that shifts between prey-type specializations
²⁵ are linked to shifts in tentillum and nematocyst size and shape. We found that predatory

26 specialists can evolve into generalists, and that specialists on one prey type have directly
27 evolved into specialists on other prey types. With changes in trophic niche regimes, both
28 trait optima and trait correlation patterns showed significant shifts. Thus, the evolutionary
29 history of tentilla shows that siphonophores are an example of ecological niche diversification
30 via morphological innovation and evolution. This study contributes to understanding how
31 morphological evolution has shaped present-day oceanic food webs.

32 **Keywords**

33 Siphonophores, tentilla, nematocysts, predation, specialization, character evolution

34 **Introduction**

35 Most animal predators have characteristic biological tools that they use to capture and subdue
36 prey. Raptors have claws and beaks, snakes have fangs, wasps have stingers, and cnidarians
37 have nematocyst-laden tentacles. The functional morphology of these structures tends to be
38 finely attuned to their ability to successfully capture specific prey [1]. Long-term adaptive
39 evolution in response to the defense mechanisms of the prey (*e.g.* avoidance, escape, protective
40 barriers) leads to modifications that can counter those defenses. The more specialized the
41 diet of a predator is, the more specialized its tools need to be to meet the specific challenges
42 posed by the prey. Understanding the relationships between predatory and morphological
43 specializations is necessary to contextualize the phenotypic diversity of predators, and to
44 quantify the importance of ecological diversification in generating this diversity.

45 Siphonophores (Cnidaria: Hydrozoa) are a clade of organisms bearing modular structures
46 that are exclusively used for prey capture: the tentilla (Fig. 1). These present a significant
47 morphological variation across species [2] (Fig. 2), which makes them an ideal system to
48 study the relationships between functional traits and prey specialization. A siphonophore is
49 a colony bearing many feeding polyps (Fig. 1), each with a single tentacle, which branches
50 into several tentilla carrying the functional cnidocytes (specialized neural cells carrying

51 nematocysts, the stinging capsules). Unlike most other cnidarians, siphonophores carry their
52 tentacle nematocysts in extremely complex and organized batteries [3] built into their tentilla
53 (tentacle side branches). While nematocyst batteries and clusters in other cnidarians are
54 simple static scaffolds for cnidocytes, siphonophore tentilla have their own reaction mechanism,
55 triggered upon encounter with prey. When it fires, a tentillum undergoes an extremely fast
56 conformational change that wraps it around the prey, maximizing the surface area of contact
57 for nematocysts to fire on the prey [4]. In addition, some species have elaborate fluorescent
58 and bioluminescent lures on their tentilla to attract prey with aggressive mimicry [5–7].
59 Siphonophores bear four major nematocyst types in their tentacles and tentilla (Fig. 1F)..
60 The largest type, heteronemes, have open-tip tubules characterized by bearing a distinctly
61 wider spiny shaft at the proximal end of the everted tubule. These are typically found flanking
62 the proximal end of the cnidoband. The most abundant type, haplonemes, have no distinct
63 shaft, but similarly to heteronemes, their tubules have open tips and can be found in the
64 cnidoband. Both heteronemes and haplonemes bear short spines along the tubule and can be
65 toxic and penetrate the surface of some prey types. In the terminal filament, siphonophores
66 bear two other types of nematocysts, characterized by their adhesive function, closed tip
67 tubules, and lack of spines on the tubule. These are the desmonemes (a type of adhesive
68 coiled-tubule spironeme), and rhopalonemes (a siphonophore-exclusive nematocyst type with
69 wide tubules).

70 Many siphonophore species inhabit the deep pelagic ocean, which spans from ~200m to
71 the oceanic seafloor. This habitat has fairly homogeneous physical conditions and stable
72 zooplankton abundances and composition [8]. With a relatively predictable prey availability,
73 ecological theory would predict evolution to drive coexisting siphonophore lineages towards
74 specialization, increasing their feeding efficiencies and reducing interspecific competition
75 [9–11]. If this prediction holds true, we expect the prey capture apparatus morphologies of
76 siphonophores to diversify with the evolution of increasing specialization on a variety of prey
77 types in different siphonophore lineages.

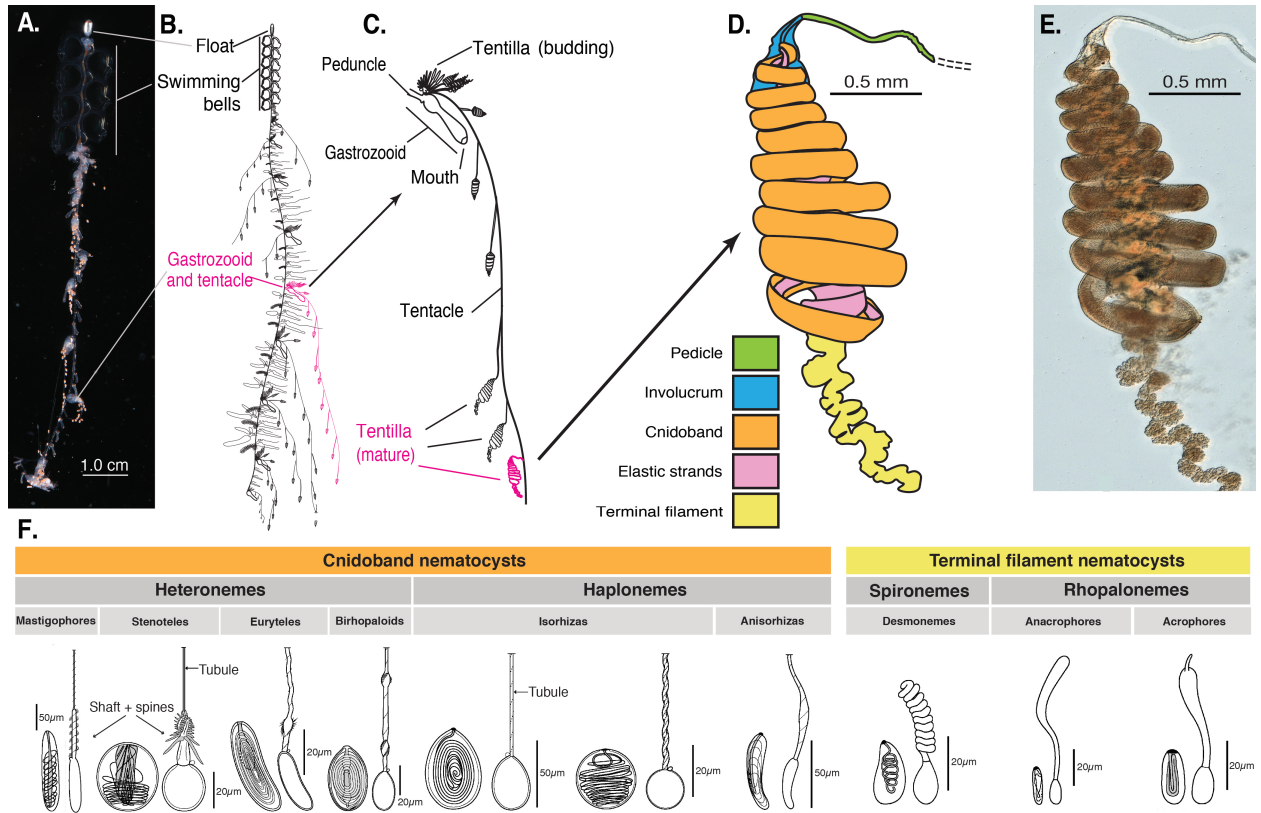


Figure 1: Siphonophore anatomy. A - *Nanomia* sp. siphonophore colony (photo by Catriona Munro). B,C - Illustration of a *Nanomia* colony, gastrozooid, and tentacle (by Freya Goetz). D - *Nanomia* sp. Tentillum illustration and main parts. E - Differential interference contrast micrograph of the tentillum illustrated in D. F - Nematocyst types (illustration reproduced with permission from Mapstone 2014), hypothesized homologies, and locations in the tentillum. Undischarged to the left, discharged to the right.

78 Specialization has been thought to be an evolutionary ‘dead-end’, meaning that specialized
79 lineages are unlikely to evolve into generalists or to shift the resource for which they are
80 specialized [12]. However, recent studies have found that interspecific competition can favor
81 the evolution of resource generalism [13–15] and resource switching [16,17]. Here we examine
82 three alternative hypotheses on siphonophore trophic specialization: (1) predatory specialists
83 evolved from generalist ancestors; (2) predatory specialists evolved from ancestral predators
84 which specialized on a different resource, switching their primary prey type; and (3) predatory
85 generalists evolved from specialist ancestors.

86 The study of siphonophore tentilla and diets has been limited in the past due to the
87 inaccessibility of their oceanic habitat and the difficulties associated with the collection of
88 fragile siphonophores. Thus, the morphological diversity of tentilla has only been characterized
89 for a few taxa, and their evolutionary history remains largely unexplored. Contemporary
90 underwater sampling technology provides an unprecedented opportunity to explore the trophic
91 ecology [18] and functional morphology [19] of siphonophores. In addition, well-supported
92 phylogenies based on molecular data are now available for these organisms [20]. These
93 advances allow for the examination of relationships between modern siphonophore form,
94 function, and ecology, as well as reconstructing their evolutionary history.

95 The few pioneering studies that have addressed the relationships between tentilla and diet
96 suggest that siphonophores are a robust system for the study of predatory specialization via
97 morphological diversification. [21] and [22] showed clear relationships between diet, tentillum,
98 and nematocyst characters in co-occurring epipelagic siphonophores. These correlations, while
99 studied for a small subset of extant epipelagic siphonophore species, might be generalizable
100 to all siphonophores. We hypothesize that these relationships reflect correlated evolution
101 between prey selection and tentillum (and nematocyst) traits. Furthermore, we hypothesize
102 that with extensive characterization of tentilla morphology, we can generate hypotheses about
103 the diets of understudied siphonophore species.

104 In this study, we characterize the morphological diversity of tentilla and their nematocysts

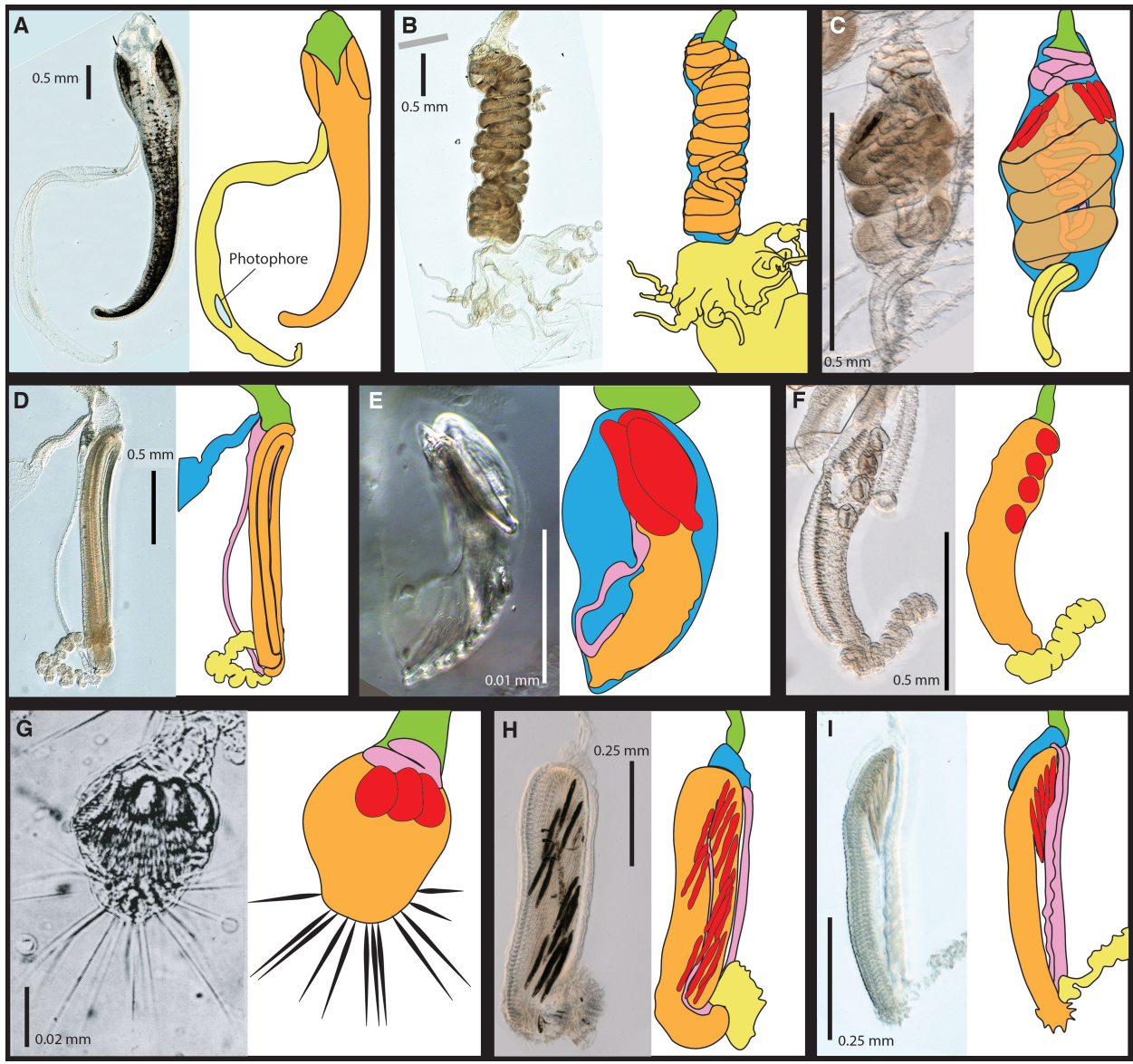


Figure 2: Tentillum diversity plate. The illustrations delineate the pedicle (green), involucrum (blue), cnidoband (orange), elastic strands (pink), terminal structures (yellow). Heteroneme nematocysts (stenoteles in C,E,F,G and mastigophores in H,I) are depicted in red for some species. A - *Erenna laciniata*, 10x. B - *Lychnagalma utricularia*, 10x. C - *Agalma elegans*, 10x. D - *Resomia ornicephala*, 10x. E - *Frillagalma vityazi*, 20x. F - *Bargmannia amoena*, 10x. G - *Cordagalma* sp., reproduced from Carré 1968. H - *Lilyopsis fluoracantha*, 20x. I - *Abylopsis tetragona*, 20x.

105 across a broad variety of shallow and deep sea siphonophore species using modern imaging
106 technologies, we expand the phylogenetic tree of siphonophores by combining a broad taxon
107 sampling of ribosomal gene sequences with a transcriptome-based backbone tree, and we
108 explore the evolutionary histories and correlations among diet, tentillum, and nematocyst
109 characters.

110 Results

111 *Phylogeny* – We built upon the published siphonophore transcriptome phylogeny [20] to pro-
112 duce tree with extensive taxonomic representation using ribosomal genes. Only 5 nodes (blue
113 dots in Figure 3) in the unconstrained inference were incongruent with the [20] transcriptome
114 tree, and these were constrained during estimation of the 18S+16S tree. The topology of
115 the constrained tree presented here (Fig. 3) is congruent with the resolved nodes in [23] and
116 [20]. However, with the unprecedented inclusion of *Stephanomia amphytridis*, this phylogeny
117 reveals a novel phylogenetic relationship between the genus *Erenna* and *Stephanomia*.

118 We retained the clade nomenclature defined in [23] and [20], such as Codonophora to
119 indicate the sister group to Cystonectae, Euphysonectae to indicate the sister group to
120 Calycophorae, Clade A and B to indicate the two main lineages within Euphysonectae. In
121 addition, we define two new clades within Codonophora (Fig. 3): Eucladophora as the
122 clade containing *Agalma elegans* and all taxa that are more closely related to it than to
123 *Apolemia lanosa*, and Tendiculophora as the clade containing *Agalma elegans* and all taxa
124 more closely related to it than to *Bargmannia elongata*. Eucladophora is characterized by
125 bearing spatially differentiated tentilla with proximal heteronemes and a narrower terminal
126 filament region. The etymology derives from the Greek *eu+kládos+phóros* for “true branch
127 bearers”. Tendiculophora are characterized by bearing rhopalonemes and desmonemes in the
128 terminal filament, having a pair of elastic strands, and developing proximally detachable
129 cnidobands. The etymology of this clade is derived from the Latin *tendicula* for “snare or
130 noose” and the Greek *phóros* for “carriers”.

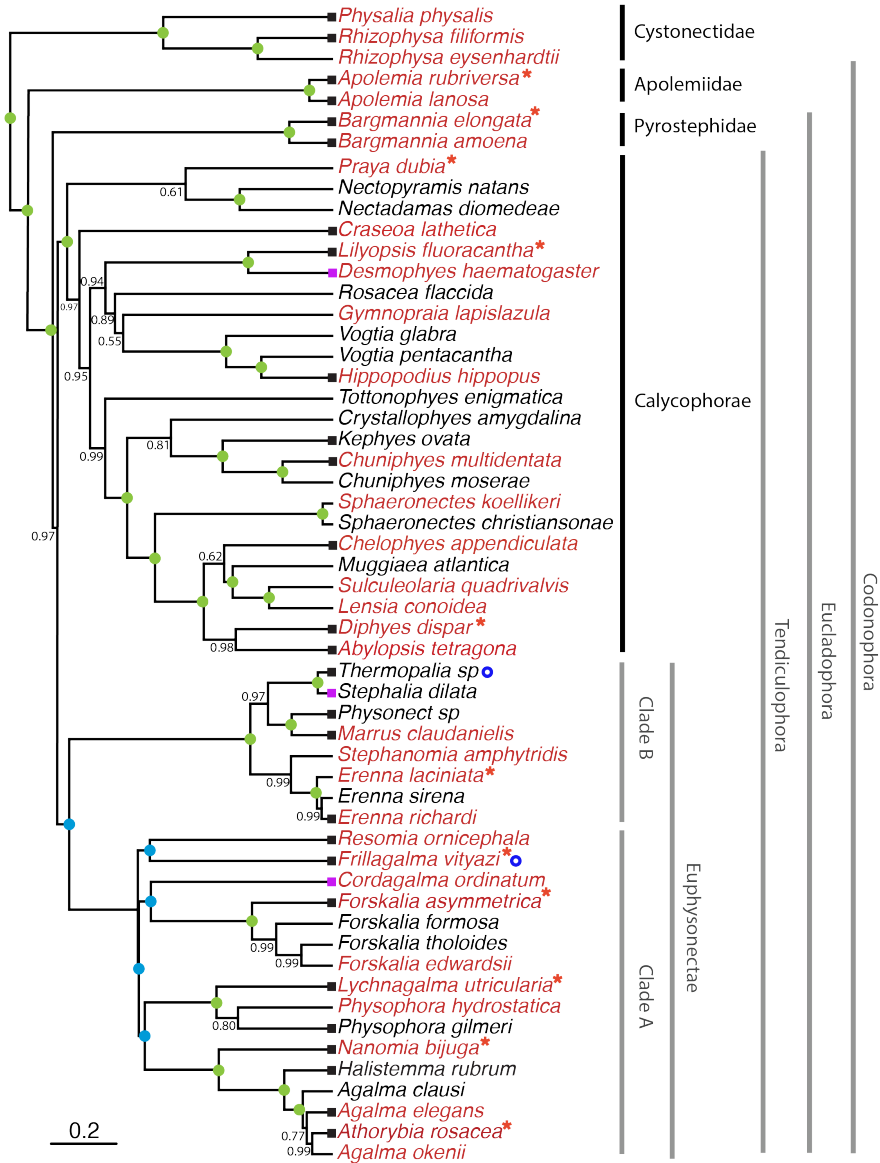


Figure 3: Bayesian time-tree built from 18S + 16S concatenated sequences. Branch lengths estimated using relaxed molecular clock. Species names in red indicate replicated representation in the morphology data. Species marked with a red asterisk were recorded using high speed video. Newly accessioned 16S data was used for species marked with a blue circle. Nodes labeled with Bayesian posteriors (BP). Green circles indicate BP = 1. Blue circles indicate nodes constrained to be congruent with (Munro *et al.* 2018). This phylogeny expands the taxon sampling of the (Munro *et al.* 2018) transcriptome tree and is congruent with it. Tips with black squares indicate the species with transcriptomes used in (Munro *et al.* 2018). Tips with grey squares indicate genus-level correspondence to taxa included in (Munro *et al.* 2018). The main clades are labeled: in black for described taxonomic units, and in grey for operational phylogenetic designations.

131 *Evolutionary associations between diet and tentillum morphology* – Reconstructions of
132 feeding guilds show that generalism is not likely to be ancestral, and it appears to have evolved
133 at least two times independently (Fig. 4). Large crustacean specialists evolve into generalists
134 twice independently, supporting hypothesis 3. Feeding guild specializations have shifted
135 from an alternative ancestral state at least five times, supporting hypothesis 2. Copepod
136 specialization and fish specialization evolved twice, and ostracod specialization evolved at
137 least once.

138 The OUwie model comparison shows that out of 30 characters, 10 show significantly
139 stronger support for the diet-driven multi-optima multi-rate OU model (SM15). These
140 characters include terminal filament nematocyst size and shape, involucrum length, elastic
141 strand width, and heteroneme number. Most of these characters are found exclusively in
142 Tendiculophora, thus this may reflect processes that could be unique to this subtree. Five
143 characters including cnidoband length, cnidoband shape, and haploneme length show maximal
144 support for a diet-driven single-optimum OU model. The remaining 15 characters support
145 BM (or OU with marginal AICc difference with BM).

146 Phylogenetic logistic regressions identified evolutionary associations between individual
147 characters and the presence of particular prey types in the diet (Fig. 4, right). Shifts toward
148 ostracod presence in diet correlated with reductions in pedicle width and total haploneme
149 volume. Shifts to copepod presence in the diet were associated with reductions in haploneme
150 width, cnidoband length and width, total haploneme and heteroneme volumes, and tentacle
151 and pedicle widths. Consistently, transitions to decapod presence in the diet correlated with
152 more coiled cnidobands (SM21).

153 Phylogenetic regressions of continuous characters against prey selectivity data produced
154 additional insights. Fish selectivity is associated with increased number of heteronemes
155 per tentillum, increased roundness of nematocysts (desmonemes and haplonemes), larger
156 heteronemes, reduced heteroneme/cnidoband length ratios, smaller rhopalonemes, lower
157 haploneme SA/V ratios, and increased size of the cnidoband, elastic strand, pedicle and

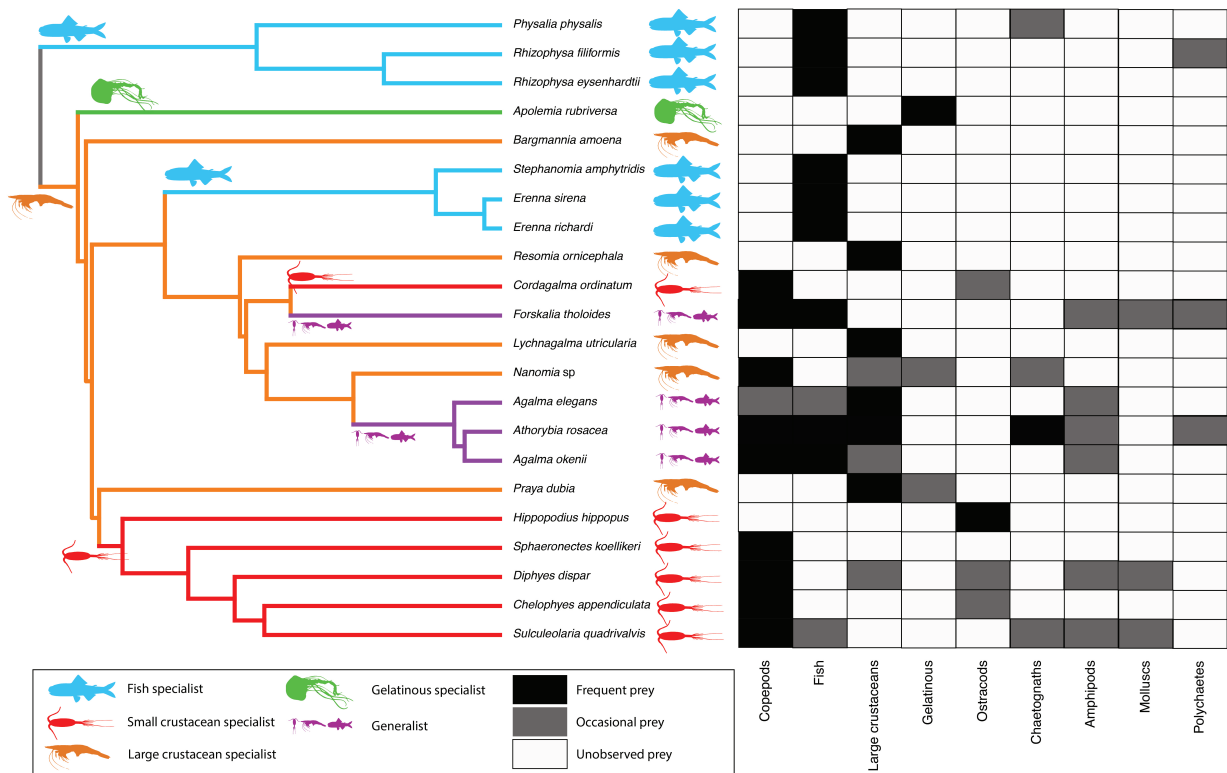


Figure 4: Left - Subset phylogeny showing the mapped feeding guild regimes that were used to inform the *OUwie* analyses. Right - Grid showing the prey items consumed from which the feeding guild categories were derived. Diet data were obtained from the literature review, available in the Dryad repository.

158 tentacle widths. Decapod-selective diets were associated with increasing cnidoband size and
159 coiledness, haploneme row number, elastic strand width, and heteroneme number. Copepod-
160 selective diets evolved in association with smaller heteroneme and total nematocyst volumes,
161 smaller cnidobands, rounder rhopalonemes, elongated heteronemes, narrower haplonemes
162 with higher SA/V ratios, and smaller heteronemes, tentacles, pedicles, and elastic strands.
163 Selectivity for ostracods was associated with reductions in size and number of heteroneme
164 nematocysts, reductions in cnidoband size, number of haploneme rows, heteroneme numbers,
165 and cnidoband coiledness. Heteroneme length and elongation also correlated negatively with
166 chaetognath selectivity (SM21).

167 When some of the diet-morphology associations reported in the literature [21,22] were
168 tested for correlated evolution (Table 1), we found that most were consistent with an
169 evolutionary explanation except the relationship between terminal filament nematocysts
170 (rhopalonemes and desmonemes) and crustaceans in the diet. The latter is likely a product
171 of the larger species richness of crustacean-eating species with terminal filament nematocysts,
172 rather than simultaneous evolutionary gains.

173 Table 1. Tests of correlated evolution between morphological characters and aspects of
174 the diet found correlated in the literature.

| Character | Aspect of diet | Test of evolutionary association | Relationship sign | P-value | Number of taxa | Association first report |
|-------------------------------|-------------------|----------------------------------|-------------------|---------|----------------|--------------------------|
| Differentiated cnidobands | Hard bodied prey | Pagel's test | + | 0.017 | 19 | Purcell, 1984 |
| Heteroneme volume | Copepod prey size | pGLS | + | 0.002 | 8 | Purcell, 1984 |
| Terminal filament nematocysts | Crustacean diet | Pagel's test | Non-Significant | 0.200 | 19 | Purcell & Mills, 1988 |
| Number of nematocyst types | Soft-bodied prey | Phylogenetic logistic regression | - | 0.040 | 22 | Purcell & Mills, 1988 |

175

176

177 *Generating dietary hypotheses using tentillum morphology* – The discriminant analysis of
178 principal components for feeding guild (7 principal components, 4 discriminants) produced
179 100% discrimination between guilds, and the highest loading contributions were found for
180 the characters (ordered from highest to lowest): Involucrum length, heteroneme volume,
181 heteroneme number, total heteroneme volume, tentacle width, heteroneme length, total
182 nematocyst volume, and heteroneme width (SM21). We used the predictions from this

discriminant function to generate hypotheses about the feeding guild of 45 species in our morphological data (SM2). This projection predicts that two other *Apolemia* species may also be gelatinous prey specialists like *Apolemia rubriversa* and that *Erenna laciniata* may be a fish specialist like *Erenna richardi*.

Table 2. Discriminant analysis of principal components for the presence of specific prey types using the morphological data. Top quartile variable (character) contributions to the linear discriminants are ordered from highest to lowest. Logistic regressions and GLMs were fitted to predict prey type presence and selectivity respectively. The sign of the slope of each predictor is reported, marked with an asterisk if significant ($p\text{-value} < 0.05$), and highlighted grey if it differs between prey presence in diet and prey selectivity. Pseudo- R^2 (%) approximates the percent variance explained by the model.

| Prey type | DAPC | GLM for prey type presence (22 taxa) | | Best fitting GLM for prey type selectivity (Purcell, 1981) (7 taxa) | |
|-------------------|------|--------------------------------------|-------------------------------------|---|-------------------|
| | | Discrimination (%) | Top quartile variable contributions | Sign | Pseudo- R^2 (%) |
| Copepods | 95.4 | Total nematocyst volume | - | -* | |
| | | Tentacle width | - | + | |
| | | Haploneme elongation | - | + | |
| | | Haploneme surface area/volume ratio | + | - | |
| | | Haploneme row number | + | + | |
| | | Cnidoband length | - | + | |
| | | Cnidoband width | - | - | |
| Fish | 68.1 | Cnidoband free length | + | + | |
| | | Total haploneme volume | - | + | |
| | | Heteroneme volume | + | - | |
| | | Total nematocyst volume | - | + | |
| | | Total heteroneme volume | - | - | |
| | | Cnidoband length | - | - | |
| | | Cnidoband free length | + | + | |
| Large crustaceans | 81.8 | Involucrum length | - | - | |
| | | Pedicle width | + | + | |
| | | Involucrum length | ++* | + | |
| | | Total heteroneme volume | - | - | |
| | | Elastic strand width | - | ++* | |
| | | Rhopaloneme length | + | + | |
| | | Heteroneme volume | + | - | |

194

195 *Phenotypic integration of the tentillum* – The quantitative characters we measured from 196 tentilla and their nematocysts are highly correlated. The results indicate that the dimensionality 197 of tentillum morphology is low, that many traits are associated with size, but that 198 nematocyst arrangement and shape are independent of it (SM4). The variance-covariance

matrices (SM36-38) are congruent with the abundant positive correlations observed among simple measurement characters in SM3. However, this analysis reveals more clearly the diagonal blocks that constitute the evolutionary modules, such as the heteroneme block, the terminal filament nematocyst block, and the cnidoband-pedicle-tentacle block. These results were not sensitive to the transformation of inapplicable states and taxon sampling. When we compared the rate covariance terms between characters across the different feeding guild regimes (SM41), we found that half (48%) of the character pairs presented significantly distinct correlation coefficients across different regimes (SM39), indicating that the mode of phenotypic integration also shifts with trophic niche. When contrasting the regime-specific rate correlation matrices to the whole-tree matrix, we were able to identify the character dependencies that are unique to each predatory niche (SM42).

Under the majority of SIMMAP outcomes, large crustaceans specialists are the ancestral regime, and all other regimes evolve from this ancestral specialization. Compared to the rate correlation matrix estimated over the whole tree, large crustacean specialists present strong negative correlations between haploneme elongation and heteroneme size, and between rhopaloneme elongation and tentillum size, as well as with involucrum length. With the appearance of generalists (*Forskalia* and the *Agalma-Athorybia* clade), terminal filament nematocyst (desmonemes and rhopalonemes) sizes became negatively correlated with the sizes of most characters, meaning that as some tentilla became larger, their individual terminal nematocysts became smaller, observed to the extreme in *Agalma*. In addition, heteroneme and rhopaloneme elongation became positively correlated with cnidoband size. When large crustacean specialists switched to small crustacean prey in *Cordagalma* and calycophorans, haploneme size became inversely correlated with heteroneme elongation, which in turn developed a strong positive relationship with tentillum size. In other words, as tentilla get smaller in this group, heteronemes get shorter and haplonemes get larger. The extremes of this gradient can be seen in *Cordagalma* and *Hippopodius*. With the evolution of fish prey specialization in cystonects and within Clade B, haploneme elongation became

negatively correlated with heteroneme elongation (signal driven by Clade B, since cystonects lack tentacular heteronemes), and the surface area to volume ratio of haploneme nematocysts switched from a strong negative relationship with cnidoband size (found in every other regime) to a positive correlation. Gelatinous specialization, albeit appearing only once in our tree, also carries a unique signature in character rate correlation shifts, with an increase in the strength of the correlation between heteroneme shape and shaft width, consistent with the appearance of birhopaloid nematocysts with swollen shafts that are likely effective at anchoring gelatinous tissue (see reference to Narcomedusae nematocysts in [22]).

The phylogenetic positions of the main categorical character shifts were reconstructed using stochastic character mapping (SM22-30) and summarized in 5. Haploneme nematocysts are likely ancestrally present in siphonophore tentacles since they are present in the tentacles of many other hydrozoans. Haplonemes first diverged into spherical isorhizas of 2 size classes in Cystonectae, and elongated anisorhizas of one size class in Codonophora. Haplonemes were likely lost in the tentacles of *Apolemia*, but retained as spherical isorhizas in other *Apolemia* tissues [24]. Similarly, while heteronemes exist in other tissues of cystonects, they appear in the tentacles of codonophorans exclusively, as birhopaloids in *Apolemia*, stenoteles in eucladophoran physonects, and microbasic mastigophores in calycophorans.

Eucladophora (the clade containing Pyrostephidae, Euphysonectae, and Calycophorae, see main text Fig. 3) encompasses most of the extant Siphonophore species (178 of 186) other than Cystonects and *Apolemia*. Innovations evolved in the stem of this group include spatially segregated heteroneme and haploneme nematocysts, terminal filaments, and elastic strands (Fig. 5). Pyrostephids evolved a unique bifurcation of the axial gastrovascular canal of the tentillum known as the “saccus” [25]. The stem to the clade Tendiculophora (clade containing Euphysonectae and Calycophorae, Fig. ??) subsequently acquired further novelties such as the desmoneme and rhopaloneme (acrophore subtype ancestral) nematocysts on the terminal filament (Fig. 5), which bears no other nematocyst type (Fig. 1). These are arranged in sets of 2 parallel rhopalonemes for each single desmoneme [3,26]. The involucrum

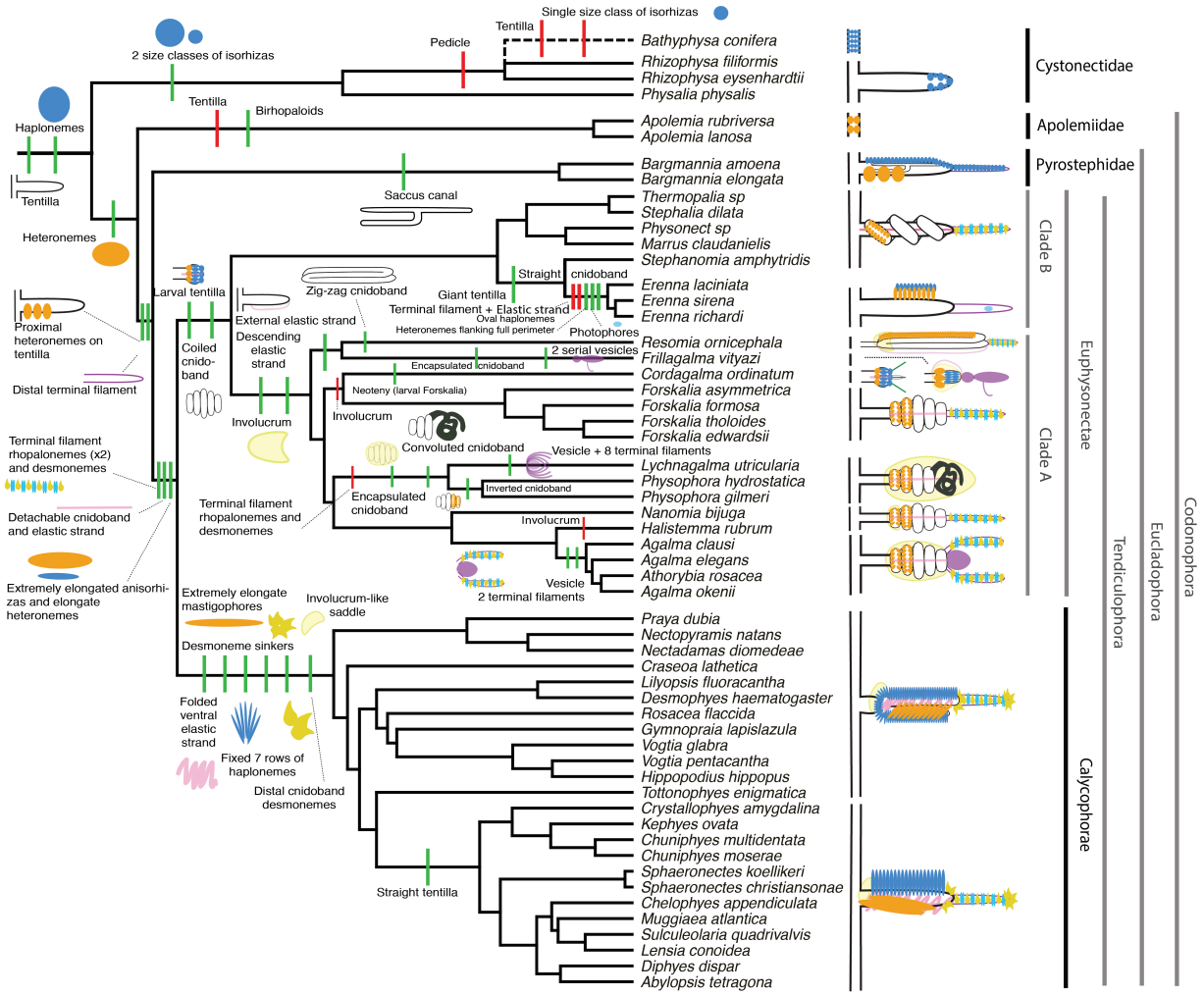


Figure 5: Siphonophore cladogram with the main categorical character gains (green) and losses (red) mapped. Some branch lengths were modified from the Bayesian chronogram to improve readability. The main visually distinguishable tentillum types are sketched next to the species that bear them, showing the location and arrangement of the main characters. In large, complex-shaped euphysonect tentilla, haplonemes were omitted for simplification. The rhizophysid *Bathyphysa conifera* branch was appended manually as a polytomy (dashed line).

253 is an expansion of the epidermal layer that can cover part or all of the cnidoband (Fig. 2).
254 This structure, together with differentiated larval tentilla, appeared in the stem branch to
255 Clade A physonects. Calycophorans evolved novelties such as larger desmonemes at the
256 distal end of the cnidoband, pleated pedicles with a “hood” (here considered homologous
257 to the involucrum) at the proximal end of the tentillum, anacrophore rhopalonemes, and
258 microbasic mastigophore-type heteronemes. While calycophorans have diversified into most
259 of the extant described siphonophore species (108 of 186), their tentilla have not undergone
260 any major categorical gains or losses since their most recent common ancestor. Nonetheless,
261 they have spread over a broad span of variation in nematocyst and cnidoband sizes.

262 *Evolution of nematocyst shape* – Haploneme nematocyst evolution has been mainly driven
263 by a single large shift towards elongation in Tendiculophora, which contains the majority of
264 described siphonophore species other than Cystonects, *Apolemia*, and Pyrostephidae. There
265 is one secondary return to more oval, less elongated haplonemes in *Erenna*, but it does not
266 reach the sphericity present in Cystonectae or Pyrostephidae (Fig. 6). Heteroneme evolution
267 presents a less discrete evolutionary history, where Tendiculophora evolved more elongate
268 heteronemes, but the difference between theirs and other siphonophores is much smaller than
269 the variation in shape within Tendiculophora, bearing no phylogenetic signal. In this clade,
270 the evolution of heteroneme shape has diverged in both directions, and there is no correlation
271 with haploneme shape (Fig. 6), which has remained fairly constant (elongation between 1.5
272 and 2.5).

273 Haploneme and heteroneme shape share 21% of their variance across extant values, and
274 53% of the variance in their shifts along the branches of the phylogeny. However, much
275 of this correlation is due to the contrast between Pyrostephidae and their sister group
276 Tendiculophora (Fig. 3). BAMM identified a regime shift in heteroneme shape evolution on
277 the branches leading to *Agalma* and *Athorybia* (SM33). For the rates of haploneme shape
278 evolution, BAMM identified two main independent regime shifts (Fig. 6): one in the branch
279 leading to Codonophora (anisorhizas diverging from cystonects’ spherical isorhizas), and one

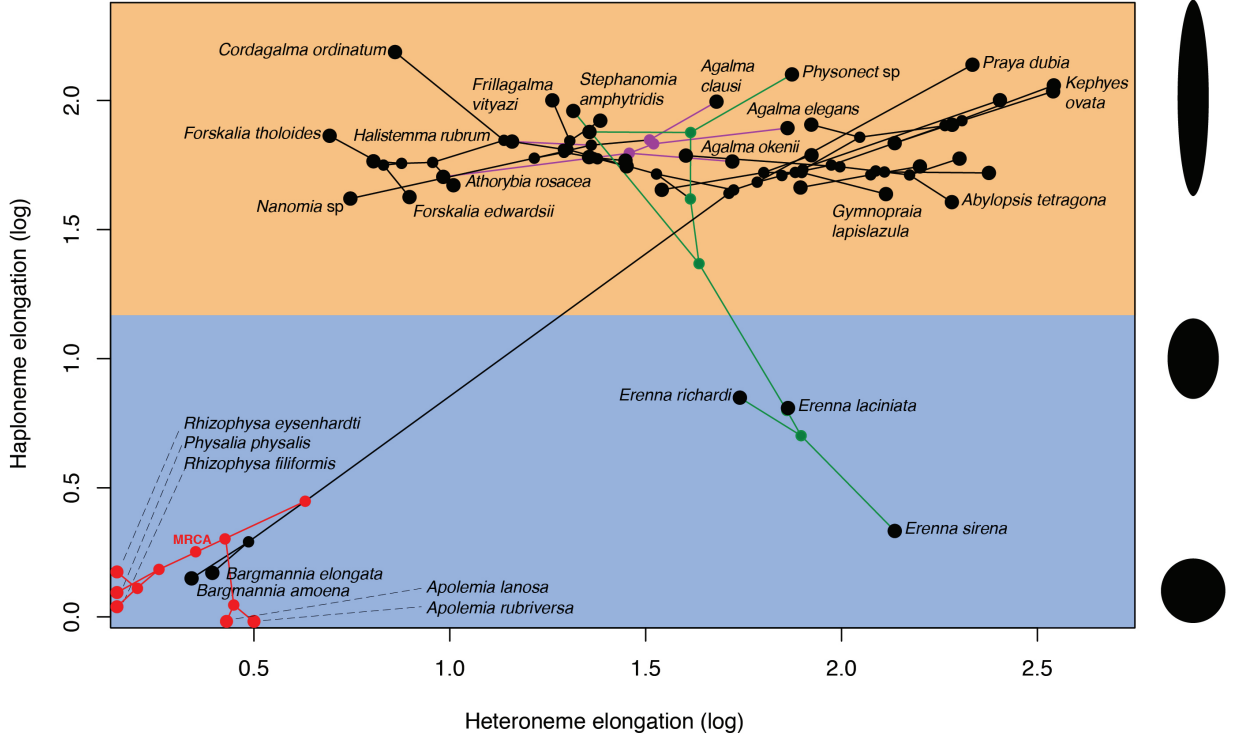


Figure 6: Phylomorphospace showing haploneme and heteroneme elongation (log scaled). Orange area delimits rod-shaped haplonemes, blue area covers oval and round-shaped haplonemes. Smaller dots and lines represent phylogenetic relationships and ancestral states of internal nodes under BM. Species nodes in red were manually added to the plot. Cystonects have no tentacle heteronemes and are projected onto the haploneme axis. Apolemiids have no tentacle haplonemes and are projected onto the heteroneme axis. Colored branches and nodes correspond to BAMM regimes of accelerated haploneme shape (green) and heteroneme shape (violet) evolution.

280 in the branch leading to Clade B physonects (SM35). Clade B includes *Erenna*, *Stephanomia*,
281 *Marrus*, and rhodaliids. Most of these taxa have rod-shaped anisorhizas, but *Erenna* has
282 oval ones). No significant regime shift patterns were identified in the evolution of desmoneme
283 and rhopaloneme shape.

284 Discussion

285 The core aims of this study are to examine the evolutionary history of siphonophore tentilla and
286 diet, characterize the evolutionary shifts in their trophic niches, and identify the morphological
287 characters that evolve with changes in prey type. We inquire whether the relationships between
288 form and function observed in extant taxa are due to correlated evolution or non-evolutionary
289 causes, whether the evolution of their trophic specializations supports or challenges traditional
290 ecological theory (such as the idea specialists evolve from generalists), and whether the diets
291 of siphonophores can be hypothesized by observing their tentacles. In addition, we produced
292 novel findings on tentillum morphology, siphonophore phylogeny, nematocyst character
293 evolution, and tentillum discharge dynamics.

294 *Evolution of tentillum morphology with diet* – Siphonophores are an abundant group of
295 zooplankton in oceanic ecosystems [27,28]. While little is known about siphonophore trophic
296 ecology, what is known indicates that they occupy a central position in midwater food webs
297 [18], serving as trophic intermediaries between smaller zooplankton and higher trophic level
298 predators. Siphonophore species have been observed to feed on a variety of prey with very
299 different sizes, traits, and behaviors. Because there is a total absence of siphonophores in
300 the fossil record, how they became established as the ubiquitous and diversified predators
301 in today’s oceans remains an open question. Predators that use morphologically similar
302 tools for prey capture tend to capture similar prey, thus their abundance and coexisting
303 species diversity are inversely related due to competitive exclusion by resource limitation
304 [29]. However, this is not consistent with what we observe in siphonophores, which have been
305 found to be both very abundant and locally diverse [27]. We hypothesize that siphonophores

306 have escaped this by specializing in different prey resources.

307 According to our reconstructions, the evolutionary history of siphonophore diets indicates
308 that being a specialist was an ancestral aspect of their trophic niche, while trophic generalism
309 is likely a derived condition. Several studies (reviewed in [12]) have suggested that resource
310 specialization is an irreversible dead-end due to the constraints posed by extreme phenotypic
311 specialization. Our reconstructions show that this is not the case for siphonophores, where
312 the prey type on which they specialize has shifted at least 5 times, and generalism has evolved
313 independently at least twice. Among the evolutionary hypotheses considered, we find support
314 for both hypotheses 2 (specialist resource switching) and 3 (specialist to generalist), but no
315 support for hypothesis 1 (generalist to specialist). This is consistent with the findings of
316 recent studies on phytophagous insects [15], where the rate of evolution from generalists to
317 specialists is comparable to the reverse, thus specialization does not limit further evolution.
318 However, [30] found that ancestral reconstruction methods can be biased, and tend to infer
319 higher transition rates toward the more frequent state. With this in mind, we should expect
320 to find a predominance of transitions from generalists to specialists (the more common
321 state across the tips). Nonetheless, we observe the opposite, indicating strong evidence that
322 these generalists are indeed a derived state. Our results are also consistent with the [17]
323 study on lepidopterans, where specialized resource switching is the primary transition type
324 while niche breadth remains fairly constant. The evolutionary history of tentilla shows that
325 siphonophores are an example of trophic niche diversification via morphological innovation
326 and evolution, which allowed transitions between specialized trophic niches. This evolutionary
327 mechanism is particularly important in a deep open ocean ecosystem, which is a relatively
328 homogeneous physical environment, where the primary niche heterogeneity available is the
329 potential interactions between organisms [8].

330 One of the most common prey items found in siphonophore diets is copepods (Fig. 4).
331 Copepod-specialized diets have evolved convergently in *Cordagalma* and some calycophorans.
332 These evolutionary transitions happened together with transitions to smaller tentilla with

333 fewer cnidoband nematocysts. Tentilla are expensive single-use structures [4], therefore we
334 would expect that specialization in small prey would beget reductions in the size of the prey
335 capture apparatus to the minimum required for the ecological performance. *Cordagalma*'s
336 tentilla strongly resemble the larval tentilla (only found in the first-budded feeding body of
337 the colony) of their sister genus *Forskalia*. This indicates that the evolution of *Cordagalma*
338 tentilla could be a case of paedomorphosis associated with predatory specialization on smaller
339 prey.

340 [21] showed that haplonemes have a penetrating function as isorhizas in cystonects and an
341 adhesive function as anisorhizas in Tendiculophora. The two clades that have been observed
342 primarily feeding on fish (Cystonectae and Clade B, which includes *Erenna*, *Stephanomia*,
343 *Marrus*, and rhodaliids) present an accelerated rate of haploneme shape evolution towards
344 more compact haplonemes, significantly distinct from their closest relatives. Isorhizas in
345 cystonects are known to penetrate the skin of fish during prey capture, and to deliver the
346 toxins that aid in paralysis and digestion [31]. *Erenna* anisorhizas are also able to penetrate
347 human skin and deliver a painful sting [32] (and pers. obs.), a common feature of piscivorous
348 cnidarians like the portuguese man-o-war or box jellies.

349 [33] hypothesized that smaller, more spherical nematocysts, with a lower surface area to
350 volume ratio, are more efficient in osmotic-driven discharge and thus have more power for
351 skin penetration. The elongated haplonemes of crustacean-eating Tendiculophora have never
352 been observed penetrating their crustacean prey ([21] and our unpublished observations),
353 and are hypothesized to entangle the prey through adhesion of the abundant spines to the
354 exoskeletal surfaces and appendages. Entangling requires less acceleration and power during
355 discharge than penetration, as it does not rely on point pressure. In fish-eating cystonects
356 and *Erenna* species, the haplonemes are much less elongated and very effective at penetration,
357 in congruence with the osmotic discharge hypothesis.

358 When we tested the diet-morphology correlation hypotheses supported in the literature
359 from a macroevolutionary perspective (Table 1), we found that most of them were consis-

360 tent with correlated evolution. The ecomorphological association between rhopalonemes,
361 desmonemes, and crustacean eaters was not congruent with a scenario of correlated evolution.
362 This is probably due to the broader set of taxa in our analyses, including multiple species
363 without desmonemes or rhopalonemes but which effectively capture crustaceans (such as
364 *Cordagalma ordinatum*, *Lychnagalma utricularia*, and *Bargmannia amoena*).

365 Our work identifies an interesting example of convergent evolution. The region of the
366 tentillum morphospace (SM4) occupied by calycophorans was independently (and more
367 recently) occupied by the physonect *Frillagalma vityazi*. Like calycophorans, *Frillagalma*
368 tentilla have small C-shaped cnidobands with a few rows of anisorhizas. Unlike calycophorans,
369 they lack paired elongate microbasic mastigophores. Instead, they bear exactly three oval
370 stenoteles, and their cnidobands are followed by a branched vesicle, unique to this genus.
371 Their tentillum morphology is very different from that of other related physonects, which
372 tend to have long, coiled, cnidobands with many paired oval stenoteles. Most studies on
373 calycophoran diets have reported their prey to be primarily composed of small crustaceans,
374 such as copepods or ostracods [21,34]. The diet of *Frillagalma vityazi* is unknown, but this
375 morphological convergence suggests that they evolved to capture similar kinds of prey. Our
376 DAPCs (SM16-20) predict that *Frillagalma* has a generalist niche with both soft and hard
377 bodied prey, including copepods.

378 While our results unambiguously show that tentillum morphology evolved with diet, the
379 conclusions we can draw from these analyses are limited by the sparse dietary data available.
380 Moreover, our analyses are not sufficient to adequately test hypotheses of adaptation, since
381 that would require evidence of changes within a population exposed to different selective
382 pressures. When interpreting these results, it is important to remember that diet is a product
383 of environmental prey availability and predator selectivity. Selectivity differences across
384 siphonophore species could be driven by other phenotypes not accounted for this study. For
385 example, tentacle-deploying behavior, positioning in the water column, sensitivity thresholds
386 for nematocyst discharge, or chemical cues to ingest a captured animal. Further observations

387 on these behaviors in the field are necessary to assess their relative importance in determining
388 dietary composition. In addition to behavior, there is much biochemistry in the prey capture
389 and digestion processes that remains unexplored. Part of the success in siphonophore prey
390 capture is likely determined by the effectiveness of the toxins delivered by the nematocysts
391 on different taxa. Comparative toxin assays and venom protein evolution studies would
392 shed light on this question. Moreover, siphonophore trophic specialization may have brought
393 changes in the digestive biochemistry of gastrozooids and palpons. A comparison of the gene
394 expression levels for different enzymes in the gastrozooids of different species, together with
395 digestive enzyme sequence evolution studies, and a toxicological assay of the different venoms
396 in siphonophore nematocysts on different prey taxa, would provide a great complement to
397 our results.

398 *Phenotypic integration of siphonophore tentilla* – Many tentillum characters, such as
399 nematocysts, arose from the subfunctionalization of serial homologs [35]. Serial homologs have
400 shared genetic elements underlying their development, and are expected to have phylogenetic
401 correlations [36]. In addition, these sub-structures must fit and work together in synchrony
402 to ensnare prey successfully (functional integration). Character complexes that satisfy these
403 conditions tend to be phenotypically integrated. Phenotypic integration is the set of functional
404 and genetic correlations among the traits of an organism [37]. These correlations have been
405 hypothesized to direct and constrain adaptive evolution [36]. The siphonophore tentillum
406 morphospace has a fairly low extant dimensionality due to having an evolutionary history with
407 many synchronous, correlated changes. This is consistent with strong phenotypic integration
408 where genetic and developmental correlations are maintained by natural selection to preserve
409 a complex function across the wide variety of morphologies tentilla can present.

410 Structural correlations within the tentillum are expected without the need to invoke
411 natural selection, since most characters develop from a common bud (budding tentilla near
412 the base of the tentacle). Similarly, correlations between nematocyst subtypes are also
413 expected given their common evolutionary and developmental origin [35,38]. However, we

414 also found correlations between nematocyst and tentillum characters. Siphonophore tentacle
415 nematocysts (in their cnidocytes) are not produced nor matured in the developing tentillum.
416 These cnidocytes are produced by dividing cnidoblasts in the basigaster (basal swelling of
417 the gastrozooid). Once the cnidocytes have assembled the nematocyst, they migrate outward
418 along the tentacle [39] and position themselves in the tentillum according to their type and size
419 [3]. Thus, the developmental programs that produce the observed nematocyst morphologies
420 are spatially separated from those producing the tentillum morphologies. Therefore, we
421 hypothesize the genetic correlations and phenotypic integration between tentillum and
422 nematocyst characters are maintained through natural selection on separate regulatory
423 networks, out of the necessity to work together and meet the spatial, mechanical, and
424 functional constraints of their prey capture behavior.

425 Our evolutionary rate covariance results indicate that tentilla are not only phenotypically
426 integrated but also show patterns of evolutionary modularity, where different sets of characters
427 appear to evolve in stronger correlations among each other than with other characters. This
428 may be indicative of the underlying genetic and developmental dependencies among closely
429 homologous nematocyst types (such as desmonemes and rhopalonemes) and structures. In
430 addition, these evolutionary modules point to hypothetical functional modules. For example,
431 the coiling degree of the cnidoband and the extent of the involucrum have correlated rates of
432 evolution, while high-speed videos show that the involucrum helps direct the whiplash of the
433 uncoiling cnidoband forward (towards the prey).

434 While selection acting on character states is a widely studied phenomenon, recent studies
435 have shown that selection can also act upon the patterns of character correlations and
436 phenotypic dependencies [40–46]. This evolution of character relationships can allow lineages
437 to explore new regions of the morphospace and facilitate the appearance of ecological
438 novelties. Our results show that the patterns of phenotypic integration in siphonophore
439 tentilla vary among clades, and appear to display different relationships across shifting feeding
440 specializations. Similarly to what has been found in the feeding morphologies of fish [42,47],

⁴⁴¹ siphonophore tentilla may have accommodated new diets by altering the correlations between
⁴⁴² characters. For example, changes in the size and shape relationships between nematocyst
⁴⁴³ types gave rise to the nematocyst complements specialized in ensnaring prey with different
⁴⁴⁴ combinations of defensive traits. Finally, the evolvability of phenotypic dependencies likely
⁴⁴⁵ had a large role in the evolution of the diverse tentilla morphologies we observe today across
⁴⁴⁶ siphonophores.

⁴⁴⁷ *Evolution of nematocyst shape* – The phylogenetic placement of siphonophores among
⁴⁴⁸ the Hydrozoa remains an unresolved question [20]. The most recent work on this front sets
⁴⁴⁹ them as the sister group to all other Hydroidolina [48]. Therefore, there is great uncertainty
⁴⁵⁰ around the ancestral plesiomorphies of the common ancestor of all siphonophores. This is
⁴⁵¹ especially true for those characters that present extreme differences between Cystonectae
⁴⁵² and Codonophora (the earliest split in the siphonophore phylogeny). One such character is
⁴⁵³ the shape of haploneme nematocysts. A remarkable feature of siphonophore haplonemes is
⁴⁵⁴ that they are outliers to all other Medusozoa in their surface area to volume relationships,
⁴⁵⁵ deviating significantly from sphericity [33]. This suggests a different mechanism for their
⁴⁵⁶ discharge that could be more reliant on capsule tension than on osmotic potentials [49],
⁴⁵⁷ and strong selection for efficient nematocyst packing in the cnidoband [3,33]. Our results
⁴⁵⁸ show that Codonophora underwent a shift towards elongation and Cystonectae towards
⁴⁵⁹ sphericity, assuming the common ancestor had an intermediate state. Since we know that
⁴⁶⁰ the haplonemes of other hydrozoan outgroups are generally spheroid, it is more parsimonious
⁴⁶¹ to assume that cystonects retain this ancestral state. Later, we observe a return to more
⁴⁶² rounded (ancestral) haplonemes in *Erenna*, concurrent with a secondary gain of a piscivorous
⁴⁶³ trophic niche, like that exhibited by cystonects.

⁴⁶⁴ The implications of these results to the evolution of nematocyst function are that an
⁴⁶⁵ innovation in the discharge mechanism of haplonemes may have occurred during the main shift
⁴⁶⁶ to elongation. Elongate nematocysts can be tightly packed into cnidobands. We hypothesize
⁴⁶⁷ this may be a Tendiculophora lineage-specific adaptation to packing more nematocysts into

468 a limited tentillum space, as suggested by [3]. Tendiculophora, comprised of the clades
469 Euphysonectae and Calycophorae, includes the majority of siphonophore species. Among
470 these, are the most abundant siphonophore species, and a greater morphological and ecological
471 diversity is found. We hypothesize that this packing-efficient haploneme morphology may have
472 been a key innovation leading to the diversification of this clade. However, other characters
473 that shifted concurrently in the stem of this clade may have been responsible for their extant
474 diversity.

475 Conclusions

476 Siphonophores have diverse predatory niches in the open ocean, ranging from mid-trophic
477 small crustacean eaters to piscivorous super-carnivores. With the evolution of diversified prey
478 type specializations comes the evolution of morphologies adapted to the challenges posed
479 by different prey. The results presented here indicate that the associations found between
480 siphonophore tentilla and their prey are a product of correlated evolution in highly integrated
481 traits. While much of the literature focuses on how predatory generalists evolve into predatory
482 specialists, in siphonophores we find predatory specialists can evolve into generalists, and that
483 specialists on one prey type have directly evolved into specialists on other prey types. We
484 find that the evolutionary optima and genetic correlations of many tentillum characters have
485 evolved following these shifts in trophic niche. Our extended morphological characterization
486 shows that the relationships between form and ecology hold across a large set of taxa and
487 characters, and can be used to generate hypotheses on the feeding habits of uncharacterized
488 species. In light of these results, we conclude that the evolutionary diversification of tools for
489 prey capture contributed to the diversification of trophic interactions. Therefore, we identify
490 organismal trait evolution as a key driver in the emergence of food web complexity.

491 Materials and Methods

492 *Tentillum morphology* – The morphological work was carried out on siphonophore specimens
493 fixed in 4% formalin from the Yale Peabody Museum Invertebrate Zoology (YPM-IZ) collection
494 (accession numbers in Dryad repository). These specimens were collected intact across many
495 years of fieldwork expeditions, using blue-water diving [50], remotely operated vehicles (ROVs),
496 and human-operated submersibles. Tentacles were dissected from non-larval gastrozooids,
497 sequentially dehydrated into 100% ethanol, cleared in methyl salicylate, and mounted onto
498 slides with Canada Balsam or Permount mounting media. The slides were imaged as tiled
499 z-stacks using differential interference contrast (DIC) on an automated stage at YPM-IZ
500 (with the assistance of Daniel Drew and Eric Lazo-Wasem) and with laser point confocal
501 microscopy using a 488 nm Argon laser that excited autofluorescence in the tissues. Thirty
502 characters (defined in SM5) were measured using Fiji [51,52]. We did not measure the lengths
503 of contractile structures (terminal filaments, pedicles, gastrozooids, and tentacles), since they
504 are too variable to quantify. We measured at least one specimen for 96 different species (see
505 raw data by species in Dryad). Of these, we selected 38 focal species across clades based on
506 specimen availability and phylogenetic representation. Three to five tentacle specimens from
507 each one of these selected species were measured to capture intraspecific variation.

508 *Siphonophore phylogeny* – While the main goal of this work is not to elucidate a novel
509 phylogeny for Siphonophora, we did expand on the most recent transcriptome based phylogeny
510 [20] to accommodate a larger taxon sampling. In order to do this, we ran a constrained analysis
511 on an extensive 18S+16S dataset. The phylogenetic analysis included 55 siphonophore species
512 and 6 outgroup cnidarian species (*Clytia hemisphaerica*, *Hydra circumcincta*, *Ectopleura*
513 *dumortieri*, *Porpita porpita*, *Velella velella*, *Staurocladia wellingtoni*). The gene sequences we
514 used in this study are available online (accession numbers in Dryad Repository). Some of the
515 sequences we used were accessioned in [23], and others we extracted from the transcriptomes
516 in [20]. Two new 16S sequences for *Frillagalma vityazi* (MK958598) and *Thermopalia* sp.
517 (MK958599) sequenced by Lynne Christianson using the primers from [53] (read 3' to 5' F:

518 TCGACTGTTACCAAAACATAGC , R: ACGGAATGAACCTCAAATCATGTAAG) were
519 included and accessioned to NCBI. We aligned these sequences using MAFFT [54] (alignments
520 available in Dryad). We inferred a Maximum Likelihood (ML) phylogeny (SM6) from 16S
521 and 18S ribosomal rRNA genes using IQTree [55] with 1000 bootstrap replicates (iqtree -s
522 alignment.fa -nt AUTO -bb 1000). We used ModelFinder [56] implemented in IQTree v1.5.5.
523 to assess relative model fit. ModelFinder selected GTR+R4 for having the lowest Bayesian
524 Information Criterion score. Additionally, we inferred a Bayesian tree with each gene as an
525 independent partition in RevBayes [57] (SM9 and SM11), which was topologically congruent
526 with the unconstrained ML tree. The *alpha* priors were selected to minimize prior load in
527 site variation.

528 Given the broader sequence sampling of the transcriptome phylogeny, we ran constrained
529 inferences (using both ML and Bayesian approaches, which produced fully congruent topologies
530 (SM8 and SM10)) after fixing the 5 nodes that were incongruent with the topology of the
531 consensus tree in [20]. This topology was then used to inform a Bayesian relaxed molecular
532 clock time-tree in RevBayes, using a birth-death process (sampling probability calculated
533 from the known number of described siphonophore species) to generate ultrametric branch
534 lengths (SM11-12). Scripts available in the Dryad repository.

535 *Feeding ecology* – We extracted categorical diet data for different siphonophore species
536 from published sources, including seminal papers [4,21,34,58–61], and ROV observation data
537 [18,62] with the assistance of Elizabeth Hetherington and C. Anela Choy (available in Dryad
538 repository). We removed the gelatinous prey observations for *Praya dubia* eating a ctenophore
539 and a hydromedusa, and for *Nanomia* sp. eating *Aegina*, since we believe these are rare events
540 that have a much larger probability of being detected by ROV methods than their usual prey,
541 and it is not clear whether the medusae were attempting to prey upon the siphonophores.
542 Personal observations on feeding (from SHDH, CAC, and Philip Pugh) were also included for
543 *Resomia ornicephala*, *Lychnagalma utricularia*, *Bargmannia amoena*, *Erenna richardi*, *Erenna*
544 *laciniata*, *Erenna sirena*, and *Apolemia rubriversa*. In order to detect coarse-level patterns in

545 the feeding habits, the data were merged into feeding guilds. The feeding guilds described here
546 are: small-crustacean specialist (feeding mainly on copepods and ostracods), large crustacean
547 specialist (feeding on large decapods, mysids, or krill), fish specialist (feeding mainly on
548 actinopterygian larvae, juveniles, or adults), gelatinous specialist (feeding mainly on other
549 siphonophores, medusae, ctenophores, salps, and/or doliolids), and generalist (feeding on
550 a combination of the aforementioned taxa, without favoring any one prey group). These
551 were selected to minimize the number of categories while keeping the most different types
552 of prey separate. We extracted copepod prey length data from [21]. To calculate specific
553 prey selectivities, we extracted quantitative diet and zooplankton composition data from
554 [34], matched each diet assessment to each prey field quantification by site, calculated Ivlev's
555 electivity indices [63], and averaged those by species (data available in Dryad repository).

556 *Statistical analyses* – For subsequent comparative analyses, we removed species present in
557 the tree but not represented in the morphology data, and *vice versa*. Although we measured
558 specimens labeled as *Nanomia bijuga* and *Nanomia cara*, we are not confident in some of the
559 species-level identifications, and some specimens were missing diagnostic zooids. Thus, we
560 decided to collapse these into a single taxonomic concept (*Nanomia* sp.). All *Nanomia* sp.
561 observations were matched to the phylogenetic position of *Nanomia bijuga* in the tree. We
562 carried out all phylogenetic comparative statistical analyses in the programming environment
563 R [64], using the Bayesian ultrametric species tree (Fig. 3), and incorporating intraspecific
564 variation estimated from the specimen data as standard error whenever the analysis tool
565 allowed it. R scripts and summarized species-collapsed data available in the Dryad repository.
566 For each character (or character pair) analyzed, we removed species with missing data and
567 reported the number of taxa included. We tested each character for normality using the
568 Shapiro-Wilk test [65], and log-transformed those that were non-normal.

569 We fitted different models generating the observed data distribution given the phylogeny
570 for each continuous character using the function fitContinuous in the R package *geiger* [66].
571 The models compared were the white noise (WN; non-phylogenetic model that assumes all

572 values come from a single normal distribution with no covariance structure among species),
573 the Brownian Motion (BM) model of neutral divergent evolution [67], the Early Burst (EB)
574 model of decreasing rate of evolutionary change [68], and the Ornstein-Uhlenbeck (OU) model
575 of stabilizing selection around a fitted optimum state [69,70]. We then ranked the models in
576 order of increasing parametric complexity (WN,BM,EB,OU), and compared the corrected
577 Akaike Information Criterion (AICc) support scores [71] to the lowest (best) score, using a
578 cutoff of 2 units to determine significantly better support. When the best fitting model was
579 not significantly better than a less complex alternative, we selected the least complex model
580 (SM13). We calculated model adequacy scores using the R package *arbutus* [72] (SM14). We
581 calculated phylogenetic signal in each of the measured characters using Blomberg's K [73]
582 (SM13). We reconstructed ancestral states using Maximum Likelihood (R *phytools*::anc.ML
583 [74]), and stochastic character mapping (R *phytools*::make.simmap) for categorical characters.
584 R scripts available in Dryad.

585 In order to study the evolution of predatory specialization, we reconstructed components
586 of the diet and prey selectivity on the phylogeny using ML (R *phytools*::anc.ML). To identify
587 evolutionary associations of diet with tentillum and nematocyst characters, we compared the
588 performance of a neutral evolution model to that of a diet-driven directional selection model.
589 First, we collapsed the diet data into the five feeding guilds mentioned above (fish specialist,
590 small crustacean specialist, large crustacean specialist, gelatinous specialist, generalist), based
591 on which prey types they were observed consuming most frequently. Then, we reconstructed
592 the feeding guild ancestral states using the ML function ace (package *ape* [75]), removing tips
593 with no feeding data. The ML reconstruction was congruent with the consensus stochastic
594 character mapping (SM31). Then, using the package *OUwie* [76], we fitted an OU model with
595 multiple optima and rates of evolution matched to the reconstructed ancestral diet regimes,
596 a single optimum OU model, and a BM null model, inspired by the analyses in [77]. Finally,
597 we compared their AICc support values to select the best fitting model (SM15).

598 To model the evolutionary associations between individual tentillum and nematocyst

599 characters and the ability to capture particular prey types in the diet, we ran a series
600 of phylogenetic generalized linear models (R `phyglm::phyloglm`) (SM21). In addition, we
601 ran a series of comparative analyses to address hypotheses of diet-tentillum relationships
602 posed in the literature. To test for correlated evolution among binary characters, we used
603 Pagel's test [78]. To characterize and evaluate the relationship between continuous characters,
604 we used phylogenetic generalized least squares regressions (PGLS) [79]. To compare the
605 evolution of continuous characters with categorical aspects of the diet, we carried out a
606 phylogenetic logistic regression (R `nlme::gls` using the 'corBrownian' function for the argument
607 'correlation').

608 In order to study correlations between the rates of evolution between different characters,
609 we fitted a set of evolutionary variance covariance matrices [42] (R `phytools::evol.vcv`). When
610 fitting all covariance terms simultaneously (SM36-38), we selected the largest set of characters
611 that would allow the analysis to run without computational singularities. This excluded many
612 of the morphometric characters which are linearly dependent on other characters. Since the
613 functions do not tolerate missing data, we ran the analyses in two ways: One including all taxa
614 but transforming absent states to zeroes, and another removing the taxa with absent states.
615 To test whether phenotypic integration changes across selective regimes determined by the
616 reconstructed feeding guilds, we carried out character-pairwise variance covariance analysis
617 comparing alternative models (R `phytools::evolvcv.lite`), including those where correlations
618 are the same across the whole tree and models where correlations differ between selective
619 regimes (SM42). These analyses could only be carried out on the subset of taxa for which diet
620 data is available, and only among character pairs that are not computationally singular for
621 that taxonomic subset. Finally, we compared regime-specific variance covariance matrices to
622 the general matrix and to their preceding regime matrix to identify the changes in character
623 dependence unique to each regime (SM43). Gelatinous specialist correlations could only be
624 estimated for a small subset of characters present in *Apolemia*, and should be interpreted
625 with care.

626 To generate hypotheses about the diets of understudied siphonophores for which no
627 feeding observations have yet been reported (but for which we have tentacle morphology
628 data), we carried out linear discriminant analysis of principal components (DAPC) using
629 the dapc function (R adegenet::dapc) [80]. This function allowed us to incorporate more
630 predictors than individuals. We generated discriminant functions for feeding guild, soft/hard
631 bodied prey, and for the presence of copepods, fish, and shrimp (large crustaceans) in the
632 diet (SM16-20). From these DAPCs we obtained the highest contributing morphological
633 characters to the discriminaton (characters in the top quartile of the weighted sum of the
634 linear discriminant loadings controlling for the eigenvalue of each discriminant). For each
635 DAPC we generated hypotheses about the diets of siphonophores outside the training set
636 (R adegenet::predict.dapc), incorporating prediction uncertainty as posterior probabilities
637 (SM16-20). In order to identify the sign of the relationship between the predictor characters
638 prey type presence in the diet, we then generated generalized logistic regression models (as
639 a type of generalized linear model, or GLM using R stats::glm) with the top contributing
640 characters (from the corresponding DAPC) as predictors. We also carried out these GLMs
641 on the Ivlev's selectivity indices for each prey type calculated from [34]. Additional details
642 on the optimization are available in the Supplementary Materials.

643 To test how many times extreme nematocyst morphologies evolved, we reconstructed
644 the ancestral states of $\log(\text{length}/\text{width})$ of the different cnidoband nematocyst types, and
645 identified the branches with the greatest shifts. In addition to characterizing the shifts in the
646 state values of haploneme and heteroneme elongation, we identified and located regime shifts
647 for the rate of evolution using a Bayesian Analysis of Macroevolutionary Mixtures (BAMM)
648 [81] (SM32-35).

649 Supplementary Materials

650 Data available from the Dryad Digital Repository: <http://dx.doi.org/10.5061/dryad.NNNN>
651 Supplementary Materials are available in https://github.com/dunnlab/tentilla_morph/

652 Supplement_forShort.pdf

653 **Funding**

654 This work was supported by the Society of Systematic Biologists (Graduate Student Award
655 to A.D.S.); the Yale Institute of Biospheric Studies (Doctoral Pilot Grant to A.D.S.); and
656 the National Science Foundation (Waterman Award to C.W.D., and NSF-OCE 1829835 to
657 C.W.D., S.H.D.H., and C. Anela Choy). A.D.S. was supported by a Fulbright Spain Graduate
658 Studies Scholarship.

659 **Acknowledgements**

660 We wish to thank the crew and scientists of the R/V Western Flyer, who participated in
661 the collection of many of the specimens used in this study. We also want to thank Lynne
662 Christianson and Shannon Johnson from the Monterey Bay Aquarium Research Institute
663 for their assistance in the field as well as for sequencing some of the species included in this
664 phylogeny. In addition, we wish to thank Lourdes Rojas, Daniel Drew, and Eric Lazo-Wasem
665 for their assistance in imaging the fixed specimens and managing the collections. We thank
666 Dennis Pilarczyk for organizing the prey selectivity data, Michael Landis for helping design
667 the Bayesian analyses, and Joaquin Nunez for reviewing this manuscript. Furthermore, we
668 thank Elizabeth D. Hetherington and C. Anela Choy for collating the data on siphonophore
669 feeding and for reviewing the manuscript. Finally, we thank Philip Pugh, who confirmed
670 many of our specimen identifications and taught us valuable knowledge about siphonophores.

671 **References**

- 672 1. Schmitz O. Predator and prey functional traits: Understanding the adaptive machinery
673 driving predator–prey interactions. *F1000Research*. 2017;6.
- 674 2. Mapstone GM. Global diversity and review of siphonophorae (cnidaria: Hydrozoa).

- 675 PLoS One. 2014;9: e87737.
- 676 3. Skaer R. The formation of cnidocyte patterns in siphonophores. Academic Press New
677 York; 1988.
- 678 4. Mackie GO, Pugh PR, Purcell JE. Siphonophore Biology. Advances in Marine Biology.
679 1987;24: 97–262.
- 680 5. Purcell JE. Influence of siphonophore behavior upon their natural diets: Evidence for
681 aggressive mimicry. Science. 1980;209: 1045–1047.
- 682 6. Haddock SH, Dunn CW, Pugh PR, Schnitzler CE. Bioluminescent and red-fluorescent
683 lures in a deep-sea siphonophore. Science. 2005;309: 263–263.
- 684 7. Haddock SH, Dunn CW. Fluorescent proteins function as a prey attractant: Experi-
685 mental evidence from the hydromedusa *olindias formosus* and other marine organisms. Biology
686 open. 2015;4: 1094–1104.
- 687 8. Robison BH. Deep pelagic biology. Journal of experimental marine biology and ecology.
688 2004;300: 253–272.
- 689 9. Simpson GG. Tempo and mode in evolution. Columbia University Press; 1944.
- 690 10. Hardin G. The competitive exclusion principle. science. 1960;131: 1292–1297.
- 691 11. Hutchinson GE. The paradox of the plankton. The American Naturalist. 1961;95:
692 137–145.
- 693 12. Futuyma DJ, Moreno G. The evolution of ecological specialization. Annual review of
694 Ecology and Systematics. 1988;19: 207–233.
- 695 13. Stireman-III JO. The evolution of generalization? Parasitoid flies and the perils of
696 inferring host range evolution from phylogenies. Journal of evolutionary biology. 2005;18:
697 325–336.
- 698 14. Johnson KP, Malenke JR, Clayton DH. Competition promotes the evolution of host
699 generalists in obligate parasites. Proceedings of the Royal Society B: Biological Sciences.
700 2009;276: 3921–3926.
- 701 15. Nosil P. Transition rates between specialization and generalization in phytophagous

- 702 insects. *Evolution*. 2002;56: 1701–1706.
- 703 16. Hoberg EP, Brooks DR. A macroevolutionary mosaic: Episodic host-switching,
704 geographical colonization and diversification in complex host–parasite systems. *Journal of*
705 *Biogeography*. 2008;35: 1533–1550.
- 706 17. Hardy NB, Otto SP. Specialization and generalization in the diversification of
707 phytophagous insects: Tests of the musical chairs and oscillation hypotheses. *Proceedings of*
708 *the Royal Society B: Biological Sciences*. 2014;281: 20132960.
- 709 18. Choy CA, Haddock SH, Robison BH. Deep pelagic food web structure as revealed
710 by in situ feeding observations. *Proceedings of the Royal Society B: Biological Sciences*.
711 2017;284: 20172116.
- 712 19. Costello JH, Colin SP, Gemmell BJ, Dabiri JO, Sutherland KR. Multi-jet propulsion
713 organized by clonal development in a colonial siphonophore. *Nature communications*. 2015;6:
714 8158.
- 715 20. Munro C, Siebert S, Zapata F, Howison M, Serrano AD, Church SH, et al. Improved
716 phylogenetic resolution within siphonophora (cnidaria) with implications for trait evolution.
717 *Molecular Phylogenetics and Evolution*. 2018.
- 718 21. Purcell JE. The functions of nematocysts in prey capture by epipelagic siphonophores
719 (coelenterata, hydrozoa). *The Biological Bulletin*. 1984;166: 310–327.
- 720 22. Purcell J, Mills C. The correlation of nematocyst types to diets in pelagic hydrozoa.
721 In “the biology of nematocysts”.(Eds da hessinger and hm lenhoff.) pp. 463–485. Academic
722 Press: San Diego, CA; 1988.
- 723 23. Dunn CW, Pugh PR, Haddock SH. Molecular phylogenetics of the siphonophora
724 (cnidaria), with implications for the evolution of functional specialization. *Systematic biology*.
725 2005;54: 916–935.
- 726 24. Siebert S, Pugh PR, Haddock SH, Dunn CW. Re-evaluation of characters in apolemi-
727 idae (siphonophora), with description of two new species from monterey bay, california.
728 *Zootaxa*. 2013;3702: 201–232.

- 729 25. Totton AK, Bargmann HE. A synopsis of the siphonophora. British Museum (Natural
730 History); 1965.
- 731 26. Skaer R. Remodelling during the development of nematocysts in a siphonophore.
732 Hydrobiologia. Springer; 1991. pp. 685–689.
- 733 27. Longhurst AR. The structure and evolution of plankton communities. Progress in
734 Oceanography. 1985;15: 1–35.
- 735 28. O'Brien TD. COPEPOD, a global plankton database: A review of the 2007 database
736 contents and new quality control methodology. 2007.
- 737 29. Schluter D. Ecological character displacement in adaptive radiation. the american
738 naturalist. 2000;156: S4–S16.
- 739 30. Nosil P, Mooers A. Testing hypotheses about ecological specialization using phyloge-
740 netic trees. Evolution. 2005;59: 2256–2263.
- 741 31. Hessinger DA. Nematocyst venoms and toxins. The biology of nematocysts. Elsevier;
742 1988. pp. 333–368.
- 743 32. Pugh P. A review of the genus erenna bedot, 1904 (siphonophora, physonectae).
744 BULLETIN-NATURAL HISTORY MUSEUM ZOOLOGY SERIES. 2001;67: 169–182.
- 745 33. Thomason J. The allometry of nematocysts. The biology of nematocysts. Elsevier;
746 1988. pp. 575–588.
- 747 34. Purcell J. Dietary composition and diel feeding patterns of epipelagic siphonophores.
748 Marine Biology. 1981;65: 83–90.
- 749 35. David CN, Özbek S, Adamczyk P, Meier S, Pauly B, Chapman J, et al. Evolution
750 of complex structures: Minicollagens shape the cnidarian nematocyst. Trends in genetics.
751 2008;24: 431–438.
- 752 36. Wagner GP, Schwenk K. Evolutionarily stable configurations: Functional integration
753 and the evolution of phenotypic stability. Evolutionary biology. Springer; 2000. pp. 155–217.
- 754 37. Pigliucci M. Phenotypic integration: Studying the ecology and evolution of complex
755 phenotypes. Ecology Letters. 2003;6: 265–272.

- 756 38. Bode H. Control of nematocyte differentiation in hydra. *The biology of nematocysts*.
757 Elsevier; 1988. pp. 209–232.
- 758 39. Carré D. Study on development of cnidocysts in gastrozooids of muggiaeae kochi
759 (will, 1844) (siphonophora, calycophora). *Comptes Rendus Hebdomadaires des Seances de*
760 *l'Academie des Sciences Serie D*. 1972;275: 1263.
- 761 40. Young NM, HallgrÍmsson B. Serial homology and the evolution of mammalian limb
762 covariation structure. *Evolution*. 2005;59: 2691–2704.
- 763 41. Goswami A. Morphological integration in the carnivoran skull. *Evolution*. 2006;60:
764 169–183.
- 765 42. Revell LJ, Collar DC. Phylogenetic analysis of the evolutionary correlation using
766 likelihood. *Evolution: International Journal of Organic Evolution*. 2009;63: 1090–1100.
- 767 43. Monteiro LR, Nogueira MR. Adaptive radiations, ecological specialization, and the
768 evolutionary integration of complex morphological structures. *Evolution: International*
769 *Journal of Organic Evolution*. 2010;64: 724–744.
- 770 44. Hallgri'msson B, Jamniczky HA, Young NM, Rolian C, SCHMIDT-OTT U, Marcucio
771 RS. The generation of variation and the developmental basis for evolutionary novelty. *Journal*
772 *of Experimental Zoology Part B: Molecular and Developmental Evolution*. 2012;318: 501–517.
- 773 45. Claverie T, Patek S. Modularity and rates of evolutionary change in a power-amplified
774 prey capture system. *Evolution*. 2013;67: 3191–3207.
- 775 46. Caetano DS, Harmon LJ. Estimating correlated rates of trait evolution with uncertainty.
776 *Systematic biology*. 2018;68: 412–429.
- 777 47. Collar DC, Near TJ, Wainwright PC. Comparative analysis of morphological diversity:
778 Does disparity accumulate at the same rate in two lineages of centrarchid fishes? *Evolution*.
779 2005;59: 1783–1794.
- 780 48. Kayal E, Bentlage B, Cartwright P, Yanagihara AA, Lindsay DJ, Hopcroft RR, et al.
781 Phylogenetic analysis of higher-level relationships within hydrodolina (cnidaria: Hydrozoa)
782 using mitochondrial genome data and insight into their mitochondrial transcription. *PeerJ*.

- 783 2015;3: e1403.
- 784 49. Carré D, Carré C. On triggering and control of cnidocyst discharge. *Marine &*
785 *Freshwater Behaviour & Phy.* 1980;7: 109–117.
- 786 50. Haddock SH, Heine JN. Scientific blue-water diving. California Sea Grant College
787 Program; 2005.
- 788 51. Collins TJ. ImageJ for microscopy. *Biotechniques.* 2007;43: S25–S30.
- 789 52. Schindelin J, Arganda-Carreras I, Frise E, Kaynig V, Longair M, Pietzsch T, et al.
790 Fiji: An open-source platform for biological-image analysis. *Nature methods.* 2012;9: 676.
- 791 53. Cunningham CW, Buss LW. Molecular evidence for multiple episodes of paedo-
792 morphosis in the family hydractiniidae. *Biochemical Systematics and Ecology.* 1993;21:
793 57–69.
- 794 54. Katoh K, Misawa K, Kuma K-i, Miyata T. MAFFT: A novel method for rapid
795 multiple sequence alignment based on fast fourier transform. *Nucleic acids research.* 2002;30:
796 3059–3066.
- 797 55. Nguyen L-T, Schmidt HA, Haeseler A von, Minh BQ. IQ-tree: A fast and effective
798 stochastic algorithm for estimating maximum-likelihood phylogenies. *Molecular biology and*
799 *evolution.* 2014;32: 268–274.
- 800 56. Kalyaanamoorthy S, Minh BQ, Wong TK, Haeseler A von, Jermiin LS. ModelFinder:
801 Fast model selection for accurate phylogenetic estimates. *Nature methods.* 2017;14: 587.
- 802 57. Höhna S, Landis MJ, Heath TA, Boussau B, Lartillot N, Moore BR, et al. RevBayes:
803 Bayesian phylogenetic inference using graphical models and an interactive model-specification
804 language. *Systematic Biology.* 2016;65: 726–736.
- 805 58. Biggs DC. Field studies of fishing, feeding, and digestion in siphonophores. *Marine &*
806 *Freshwater Behaviour & Phy.* 1977;4: 261–274.
- 807 59. Pugh P, Youngbluth M. Two new species of prayine siphonophore (calycophorae,
808 prayidae) collected by the submersibles johnson-sea-link i and ii. *Journal of Plankton Research.*
809 1988;10: 637–657.

60. Bardi J, Marques AC. Taxonomic redescription of the portuguese man-of-war, physalia physalis (cnidaria, hydrozoa, siphonophorae, cystonectae) from brazil. *Iheringia Série Zoologia*. 2007;97: 425–433.
61. Andersen OGN. Redescription of marrus orthocanna (kramp, 1942)(Cnidaria, siphonophora). Zoological Museum, University of Copenhagen; 1981.
62. Hissmann K. In situ observations on benthic siphonophores (physonectae: Rhodaliidae) and descriptions of three new species from indonesia and south africa. *Systematics and Biodiversity*. 2005;2: 223–249.
63. Jacobs J. Quantitative measurement of food selection. *Oecologia*. 1974;14: 413–417.
64. Team RC. R: A language and environment for statistical computing. Vienna, austria: R foundation for statistical computing; 2017. ISBN3-900051-07-0 <https://www.R-project.org>; 2017.
65. Shapiro SS, Wilk MB. An analysis of variance test for normality (complete samples). *Biometrika*. 1965;52: 591–611.
66. Harmon LJ, Weir JT, Brock CD, Glor RE, Challenger W. GEIGER: Investigating evolutionary radiations. *Bioinformatics*. 2007;24: 129–131.
67. Martins EP. Phylogenies, spatial autoregression, and the comparative method: A computer simulation test. *Evolution*. 1996;50: 1750–1765.
68. Harmon LJ, Losos JB, Jonathan Davies T, Gillespie RG, Gittleman JL, Bryan Jennings W, et al. Early bursts of body size and shape evolution are rare in comparative data. *Evolution: International Journal of Organic Evolution*. 2010;64: 2385–2396.
69. Uhlenbeck GE, Ornstein LS. On the theory of the brownian motion. *Physical review*. 1930;36: 823.
70. Butler MA, King AA. Phylogenetic comparative analysis: A modeling approach for adaptive evolution. *The American Naturalist*. 2004;164: 683–695.
71. Sugiura N. Further analysts of the data by akaike's information criterion and the finite corrections: Further analysts of the data by akaike's. *Communications in Statistics-Theory*

- 837 and Methods. 1978;7: 13–26.
- 838 72. Pennell MW, FitzJohn RG, Cornwell WK, Harmon LJ. Model adequacy and the
839 macroevolution of angiosperm functional traits. *The American Naturalist*. 2015;186: E33–
840 E50.
- 841 73. Blomberg SP, Garland T, Ives AR. Testing for phylogenetic signal in comparative
842 data: Behavioral traits are more labile. *Evolution*. 2003;57: 717–745.
- 843 74. Revell LJ. Phytools: An r package for phylogenetic comparative biology (and other
844 things). *Methods in Ecology and Evolution*. 2012;3: 217–223.
- 845 75. Paradis E, Blomberg S, Bolker B, Brown J, Claude J, Cuong HS, et al. Package “ape”.
846 Analyses of phylogenetics and evolution, version. 2019; 2–4.
- 847 76. Beaulieu J, O’Meara B. OUwie: Analysis of evolutionary rates in an ou framework.
848 R package version 1.17. 2012.
- 849 77. Cressler CE, Butler MA, King AA. Detecting adaptive evolution in phylogenetic
850 comparative analysis using the ornstein–uhlenbeck model. *Systematic biology*. 2015;64:
851 953–968.
- 852 78. Pagel M. Detecting correlated evolution on phylogenies: A general method for the
853 comparative analysis of discrete characters. *Proceedings of the Royal Society of London*
854 Series B: Biological Sciences. 1994;255: 37–45.
- 855 79. Grafen A. The phylogenetic regression. *Philosophical Transactions of the Royal*
856 *Society of London B, Biological Sciences*. 1989;326: 119–157.
- 857 80. Jombart T, Devillard S, Balloux F. Discriminant analysis of principal components: A
858 new method for the analysis of genetically structured populations. *BMC genetics*. 2010;11:
859 94.
- 860 81. Rabosky DL, Grundler M, Anderson C, Title P, Shi JJ, Brown JW, et al. BAMM
861 tools: An r package for the analysis of evolutionary dynamics on phylogenetic trees. *Methods*
862 in *Ecology and Evolution*. 2014;5: 701–707.